CALIBRATION OF THE M_s:m_b DISCRIMINANT AT NVAR

Ileana M. Tibuleac,[1] Jessie L. Bonner,[1] Eugene T. Herrin,[2] and David G. Harkrider[3]

Weston Geophysical Corporation,[1] Southern Methodist University[2], Boston College[3]

ABSTRACT

The ability to accurately discriminate small magnitude events in areas of high monitoring concern may often rely on calibrated discriminants based upon measurements made at a single array. We are currently in the first year of a systematic evaluation of the M_s and m_b magnitude scales at NVAR (Mina, Nevada) where a broadband tripartite and short-period array will be used to help identify small amplitude Rayleigh- and P-wave motions. To date, we have initiated the data collection and NVAR m_b calibration phases of the project, and we have examined the characteristics of near-regional Rayleigh waves recorded at NVAR and MNV. Our data collection has focused on events within 20 degrees epicentral distance of NVAR that occurred between January 1999 and June 2002. We have collected waveform data from over 570 events recorded at NVAR and nearby stations, including 128 events that were only available from the archives at the Southern Methodist University Data Center. We are also analyzing the historic explosion and earthquake database for the MNV station (Denny, 1998), which is co-located with one of the broadband elements (NV31) of NVAR.

Reducing m_b bias is essential for successful application of the M_s:m_b discriminant, thus an initial research objective was to calibrate station corrections for the individual sites of the NVAR array to the body wave magnitude formula developed by Denny *et al.* (1987) at MNV. We used *Pn* and *Pg* phases from 7 events located within 13 degrees from NVAR and, using a regression of NV31 against MNV amplitudes, we estimated C=-0.01 for NV31. Using a different set of 17 earthquakes on or close to NTS we estimated C=-0.16 for NV08 and C=-1.29 for NV32. In an attempt to use the larger amplitudes of *Pg* arrivals in a formula calibrated against MNV values, we have also developed a $m_b(Pg)$ formula for events near and on NTS.

As a result of NVAR's close proximity to the Nevada Test Site, the surface waves recorded at this station from events on or near the test site are dominated by short-period Rayleigh waves with a dominant period considerably less than 20 secs. We have used phase match filtering techniques to extract Rayleigh waves from several Yucca Flat explosions, and observed that the 20 second surface waves fall below detection thresholds near m_b=4.1; however, the short-period Rayleigh waves (< 12 sec) are still measurable at m_b=3.7 and lower for explosions. These results suggest that the surface wave magnitude scale for this region must be calibrated at these shorter-periods in order to examine the performance of the M_s:m_b discriminant at smaller magnitudes.

OBJECTIVES

The ability to accurately discriminate small magnitude events in areas of high monitoring concern may often rely on a discriminant that has been calibrated for a single array or station. The objectives of this research are two-fold: The first will be a systematic evaluation and calibration of the M_s and m_b magnitude scales at NVAR (Mina, Nevada) where a broadband tripartite will be used to help properly identify small Rayleigh- wave motion. One of these broadband sites is co-located with the longstanding seismic station, MNV thus making possible the comparison of the MNV extensive historical explosion database with regional earthquakes. The second objective is to determine whether surface waves in the period band of 4 to 15 seconds can be used to accurately characterize source size. This bandwidth is considerably less than the 17 to 22 second Rayleigh waves typically used in M_s formulae. By including shorter-period surface waves in the magnitude formulae, we may be able to calculate M_s for additional near-regional events with body-wave magnitudes below 4.0 thus allowing for a thorough examination of the M_s:m_b discriminant at smaller magnitudes.

Several new regional arrays are planned for deployment during the next decade to improve capabilities for the detection, location, and discrimination of small nuclear explosions. As a result, these arrays may be within near-regional distances of known or future test sites where the performance of the M_s:m_b discriminant is not well understood. We are attempting to quantify the performance of this discriminant using near-regional data recorded at the IMS array NVAR (Figure 1) located approximately 200 km northwest of the Nevada Test Site (NTS). The array, which has been online since December 1998, consists of 10 short-period elements centered in a three-component broadband tripartite (15, 25, and 25 km legs). The northeastern station of the tripartite is collocated with station MNV, which is one of four stations in the Lawrence Livermore seismic network that has recorded most of the NTS explosions. We are currently in the initial year of the project, and we have collected our initial explosion and earthquake datasets, calibrated body wave magnitude formulae for these events in a manner consistent with Denny *et al*. (1987), and initiated research on characterizing the short-period Rayleigh waves generated on or near NTS. In the upcoming year, we will formulate the M_s scale for NVAR using the method of Marshall and Basham (1972) by calibrating distance and path dependent terms for near-regional distances and paths in this region of the western United States. Eventually, our goal will be to test the results on data recorded in other regions of monitoring concerns.
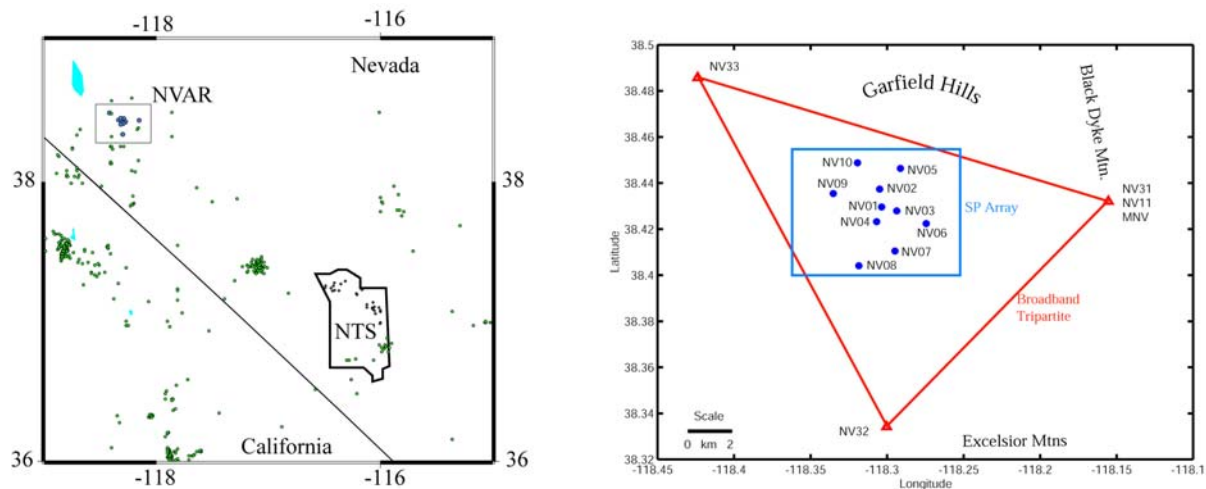

Figure 1. (Left) Map showing the location of NVAR relative to the Nevada Test Site (NTS). Also shown are the locations of regional earthquakes (green circles) recorded at NVAR since December 1998 and nuclear explosions (circles above the letters NTS) at NTS between November 1988 and September 1992. (Right) Geometry of the NVAR array including the short period (SP) elements (circles) and broadband tripartite (diamonds). The station MNV, which has recorded many of the NTS explosions, is collocated with the NV31 and NV11 stations of the NVAR array.

RESEARCH ACCOMPLISHED

Database Collection

Our data collection has focused on earthquakes within 20 degrees epicentral distance of NVAR that occurred between January 1999 and March 2002. We have collected waveform data from over 570 events recorded at NVAR and nearby stations, including 128 events that were only available from the archives at the Southern Methodist University Data Center. We have also acquired the historic explosion and earthquake database for the MNV station (Denny, 1998). Most of the events discussed in the following paper occurred on or near the Nevada Test Site (NTS) and are shown in Figure 1.

Calibration of a Regional m_b Scale at NVAR: *Pn*

The Denny *et al.* (1987) body wave magnitude formula (referred to henceforth at the DTV m_b) was specifically developed for western Unites States (US) using many events on or near NTS. They used the extensive database of earthquakes, explosions and nuclear explosions on NTS to establish a regional m_b formula at MNV, LAC, KNB, and ELK. MNV and the NVAR element NV31 are collocated (Figure 1) in the same mine and vault, thus in order to compare the historical explosions database to the new earthquake database, we calibrated the broadband elements NV31, NV32, NV33 and the short period element NV08 to the DTV m_b estimates at MNV for events on or near NTS.

We first calibrated the station dependent terms for the DTV m_b formula using the broadband and the NV08 short period elements at NVAR. The station correction, C, in their formula:

$$m_b = \log_{10}(A) + 2.4\log_{10}(\Delta) - 3.95 + C \quad (1)$$

where A is zero-to-peak amplitude in nm and Δ is the distance in km was determined to be +0.02 for MNV (Denny *et al.*, 1987). We calibrated station NV31 to compare it with the value determined for MNV. For this task, we used *Pn* and *Pg* amplitudes from 7 earthquakes that occurred during the first 3 months of 1999 (Table 1) within 3 – 13 degrees from NVAR. The events were chosen with adequate signal-to-noise (SNR) ratios and data available from both MNV and NV31.

The logarithmic plot of *Pn* (stars) and *Pg* (circles) amplitudes in nm is presented in Figure 2 for MNV (abscissa) and NV31 (ordinate). We observe a linear dependence of NV31 and MNV amplitudes and from an L2 norm fit of the data (represented as the solid line in Figure 2), we developed the following relationship:

$$\log_{10}(A_{NV31}) = 1.004\log_{10}(A_{mnv}) + 0.035. \quad (2)$$

Thus, the constant for NV31 was determined to be C_{NV31}=-0.015 in order to have the same magnitude estimates as for the station MNV.

Table 1. Events recorded at both NVAR and MNV and reported by the prototype International Data Center (pIDC). Both *Pn* and *Pg* arrivals were analyzed for events marked with *. Locations and magnitudes are from the PIDC.

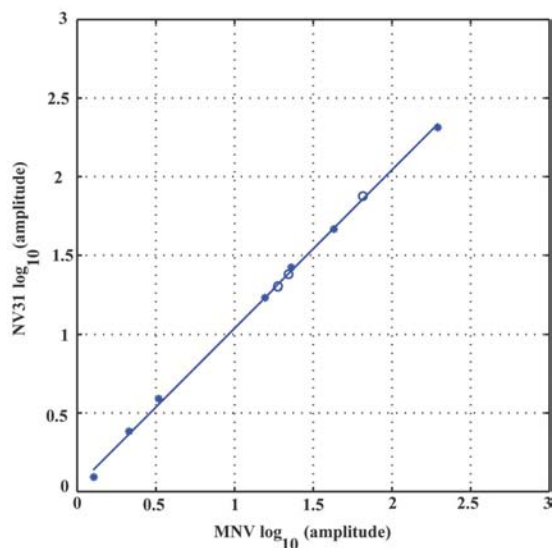| DATE	TIME	LATITUDE (DEG)	LONGITUDE (DEG)	M_B	DISTANCE (DEG)
1999/02/21*	16:50	30.93	-115.69	3.7	7.8
1999/02/24	10:02	41.30	-123.33	2.8	4.8
1999/03/09	17:48	43.32	-127.51	4.4	8.5
1999/03/13*	13:31	32.74	-116.02	3.3	6.0
1999/03/14	22:43	32.55	-104.20	3.5	12.9
1999/03/16	18:06	42.19	-125.42	4.0	6.6
1999/03/23*	18:36	36.60	-121.61	3.5	3.2

Figure 2. Amplitude estimates (nm) at NV31 as a function of MNV amplitudes (nm), for events in Table 1. Stars are first arrival measurements and open circles are *Pg* amplitude estimates.

To calculate the DTV m_b station corrections for the NV08, NV32 and NV33 stations relative to the NV31 DTV m_b, we used raw amplitude measurements from a data set of 17 events that occurred between May 1999 and June 2002 on or near NTS (Table 2). As noted from this table, we had a complete dataset for NV08, but the data availability for the broadband elements of the array is less complete. We note that NV33 was installed at a later date resulting in fewer numbers of events for analysis. For most events, the *Pn* the arrival was weak (e.g., events within 1.3 – 1.5 degrees epicentral distance, where *Pn* and *Pg* arrive within a one – two seconds time window) and in some cases only through array processing were we able to extract the *Pn* phase (Tibuleac and Herrin, 2001). Also, smaller amplitudes result in larger measurement error.

Table 2. Earthquakes near or on NTS used to calibrate Denny *et al.* (1987) magnitude formula at NV08, NV31, NV32, and NV33. Letter y shows events with *Pn* phase picks. Locations and magnitudes are by PIDC, except for events marked by stars, where locations were formed by the University of Nevada-Reno (UNR) network.

DATE	TIME	LATITUDE (DEG)	LONGITUDE (DEG)	PIDC M_B	DISTANCE (DEG)	NV08	NV31	NV32	NV33
1999/05/15	13:22	37.49	-118.62	4.7	0.97	y	y	y	
1999/05/15	13:28	37.53	-118.40	3.3	0.9	y	y	y	
1999/08/01	04:17	37.35	-117.06	3.2	1.46	y		y	
1999/08/01	16:06	37.34	-117.02	4.8	1.49	y		y	
1999/08/01	16:11	37.35	-116.91	4.2	1.54	y		y	
1999/08/01	16:26	37.40	-117.20	3.4	1.35	y		y	
1999/08/01	16:27	37.42	-116.88	4.1	1.51	y		y	
1999/08/02	05:40	37.36	-117.07	3.2	1.45	y		y	
1999/08/02	06:05	37.37	-117.02	4.5	1.47	y		y	
1999/09/26	20:11	37.36	-117.14	3.4	1.41	y	y	y	y
2000/02/28	23:08	36.00	-177.92	3.5	2.44	y	y	y	y
2000/03/02	15:00	36.08	-117.10	3.6	2.43	y	y	y	y
2002/02/19*	07:32	37.37	-117.10	3.3	1.41	y	y		
2002/03/03*	00:09	35.47	-116.48	3.0	3.29	y	y	y	y
2002/03/05*	22:23	37.37	-117.13	3.2	1.4	y	y		
2003/03/24*	10:44	37.00	-115.07	4.2	2.92	y	y		
2002/06/14*	12:40	36.71	-116.3	4.4	2.33	y	y		

In Figure 3a (upper left) we compared the corrected DTV m_b estimates at NV31 to estimates by PIDC (stars) and UNR (open circles). Observations at NV31 underestimate magnitudes for two events on NTS (distance 2.4 deg), one event at 3.2 degrees distance SE of NTS and one event near Scotty's Junction, 50 km west of NTS. However, the low magnitude estimates seem to be consistent and seen at both NV08 and NV31 (Figure 3 b) while NV32 and

NV33 do not seem to have the same behavior (Figure 3 c and d). These variations could also be the result of the complex nature of the geology of this array. The upper right and the bottom plots in Figure 3 (b,c,d) show the DTV m_b (with no station corrections) for NV08, NV32 and NV33, respectively, as a function of DTV corrected m_b at NV31 (equivalent to the MNV magnitude). L2 norm linear fits are calculated, represented by solid lines in the figures and the results are presented in Table 3. A slope close to 1 was observed between all DTV m_b values except the ones at NV33 versus NV31, possible due to the small number of estimates. Considering the value of the slopes, we calculated the DTV m_b constants for NV08 (C=-0.16) and for NV32 (C = -1.29). After applying these corrections, the L2 fits do not change, however, an L1 fit for NV08 and NV31 DTV m_b gives slopes of 0.98 (NV08 corrected DTV m_b versus NV31 corrected DTV m_b) respectively 0.97 for the same at NV32 versus NV31 The results presented in this section are preliminary as we continue to analyze events from near-regional distance to further improve the m_b calibration at NVAR.
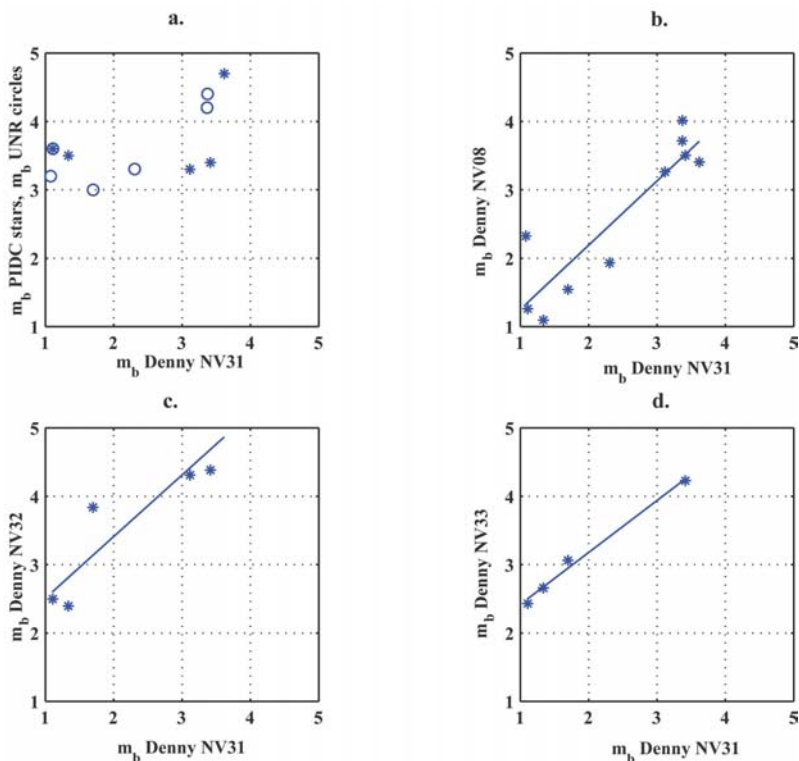

Figure 3. a) PIDC (stars) and UNR (open circles) m_b as a function of DTV m_b values, corrected to the MNV magnitude, at NV31. b) Uncorrected DTV m_b values at NV08 as a function of corrected DTV m_b at NV31 for events on or near NTS. c) Results for NV32. d) Results for NV33.

Table 3. L2 norm linear fit for NV08, NV32, NV33 (uncorrected) DTV m_b as a function of NV31 (corrected) DTV m_b and an L2 norm linear fit between NV08 and NV32

L2 NORM LINEAR FIT	FIGURE 3	NUMBER OF ESTIMATES
$m_{bNV08}(Pn) = 0.94 m_{bNV31} + 0.30$	b	10
$m_{bNV32}(Pn) = 0.90 m_{bNV31} + 1.59$	c	6
$m_{bNV33}(Pn) = 0.76 m_{bNV31} + 1.64$	d	4
$m_{bNV08}(Pn) = 0.98 m_{bNV32} - 1.18$	-	13

Calibration of a Regional m_b Scale at NVAR: *Pg*

For the events near and on the NTS that we studied, the largest arrival on the seismogram was *Pg*. In an attempt to use these larger arrivals, we have calibrated the DTV m_b for *Pg* as well, for NV08, NV31 and NV32. Figure 4a presents the values of m_b for DTV formula applied at NV31 on *Pg* the same way as on *Pn* as a function of PIDC (stars) and UNR (open circles) values. Surprisingly, these magnitudes values are closer for each event than the Pn magnitudes, even if applying the same magnitude formula for both *Pg* and *Pn* is erroneous. We have empirically calculated a formula for $m_b(Pg)$. To correct for the distance dependence, we performed a regression of the difference between the DTV magnitudes at NV31 and $\log_{10}$ of the *Pg* amplitude at all NV08, NV31, and NV32. The correction term to replace 2.44 in DTV formula was 2.72 for Pg. From *Pn* magnitude regressed against *Pg* magnitude values at NV31, we determined the following formula to obtain the equivalent of the DTV body wave magnitude using *Pg* arrivals:

$$m_b(Pg) = \log_{10}(A) + 2.72\log_{10}(\Delta) - C1 \qquad (3)$$

where A is the zero to peak Pg amplitude, Δ is the distance in km and C1 = 5.71 at NV31. The other subplots of Figure 4 present regressions of the magnitude values calculated with this formula at NV08, NV32 and NV31. The L1 norm solid lines equations are presented in Table 4. Our calculations show that C1 = 5.75 at NV08 and C1 = 6.68 at NV32. After applying the correction, the L1 fit gives a slope of 1.01 for NV32 as a function of NV31 magnitude values instead of a slope of 1.28 (see table 4).

Table 4. L1 norm linear fit for NV08, NV32, NV31 (*Pg* uncorrected) DTV m_b as a function of NV31 (*Pn* corrected) DTV m_b.

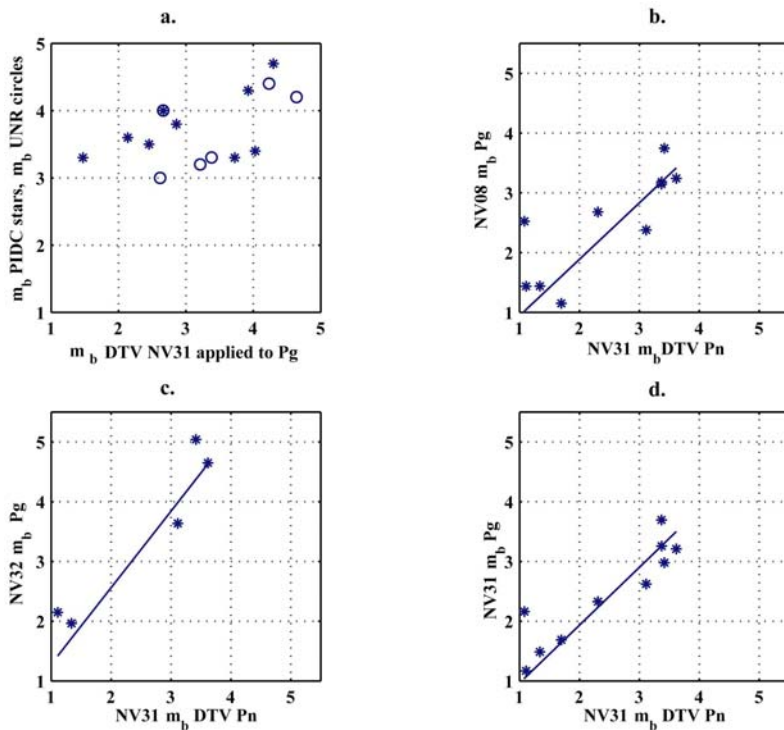| L1 NORM LINEAR FIT	FIGURE 5	NUMBER OF ESTIMATES
$m_{bNV08}(Pg) = 0.94 m_{bNV31} + 0.09$	b	10
$m_{bNV32}(Pg) = 1.28 m_{bNV31} + 0.23$	c	5
$m_{bNV31}(Pg) = 0.97 m_{bNV31} + 0.07$	d	10

Figure 4. a) PIDC and UNR magnitudes represented as a function of the NV31 DTV magnitude formula, as applied to *Pg*. (b, c, d) Formula (3) and *Pg* amplitudes were used to calculate magnitude values for NV08, NV32 and NV31, respectively, then these values were regressed against the magnitude values calculated with DTV formula for *Pn* at NV31. The solid lines are L1 fits presented in Table 4.

Characterization of Short-Period Rayleigh Waves at Near-Regional Distances

Once the m_b calibration at NVAR is completed, our research focus will shift to the development and calibration of near-regional surface wave magnitude scales. The surface waves recorded at this station from events on or near NTS (about 200 km to the SE) are dominated by short-period (< 12 sec) energy. This fact makes measurement of a conventional and stable M_s difficult, as surface wave magnitudes (Marshall and Basham, 1972; von Seggern, 1977; Vanek *et al*., 1962) are defined in the 17 to 23 second band. For example, the data from the NTS explosion TEXARKANA (2/10/89) as recorded at MNV is shown in the upper plot of Figure 5. We performed a multiple filter analyses (Dziewonski *et al*., 1969) on the data and used the resulting group velocity dispersion curve to design a phase matched filter (PMF; Herrin and Goforth, 1977) to extract the fundamental mode Rayleigh waves (lower plot of Figure 5). We then performed a narrow band-pass filter (BP 17 – 23 seconds) on the PMF extracted Rayleigh waves and the results are overlain in the lower plot of Figure 4. These data show that the 20 second surface waves for this m_b=5.2 event have amplitudes that are 8-10 dB smaller than the 7-8 second Rayleigh waves. As event size is decreased, the 20-second surface waves will fall below the detection threshold prior to the 7-8 sec energy limiting the applicability of the typical M_s measurement.
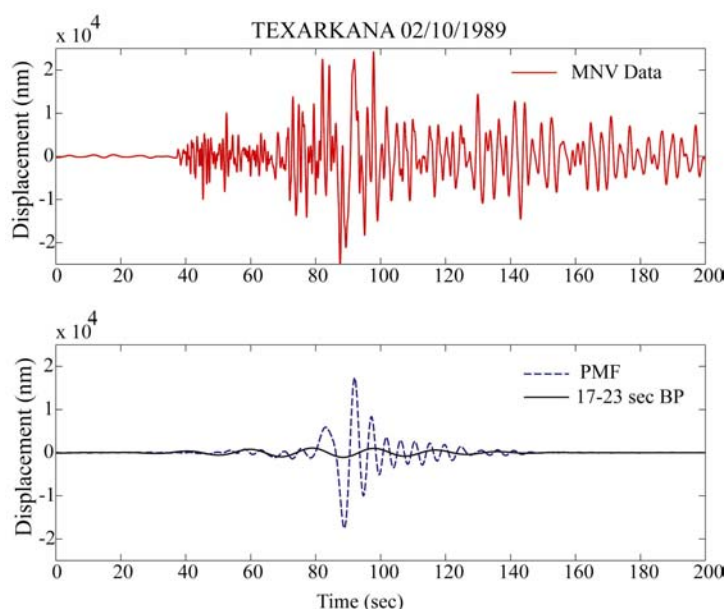

Figure 5. Waveforms from the NTS explosion TEXARKANA (Upper) recorded at station MNV. The phase match filtered Rayleigh waves (lower dashed lines) show the peak in the surface wave train corresponds to a period of 7.1 seconds and has an amplitude that is 8-10 dB larger than the surface waves in the 17 to 23 band (black line) that are typically used for measuring M_s.

These results suggest that the entire Rayleigh-wave train, not just 20-second period data, is needed for our study. Thus an initial stage of our research has been to perform the PMF technique on our explosion and earthquake datasets. For example, the PMF extracted surface waves for events from the Yucca Flats region of NTS between 1988 and 1992 are shown in Figure 6. The results show that 8 events with m_b > 4.1 had ~20 second surface waves; however, all of the events showed the 7-8 second Airy phase that dominates the propagation path from NTS to MNV (NVAR). For two events (m_b < 3.7), the largest period observed was 12.5 seconds. In addition to extracting the data, the PMF also offers enhanced signal-to-noise ratio (SNR) for dispersed Rayleigh waves as compared to routine bandpass filtering techniques. Thus, for small events in which a filter cannot be derived independently, we have derived the phase associated with a given path using the mainshock or large aftershock of an aftershock sequence. We have completed this for aftershocks from the Scotty's Junction aftershock sequence (50 km west of NTS) and extracted 5-8 second surface waves for events with m_b as small as 2.7. Cleary, developing and calibrating a M_s scale for surface wave periods less than 10 sec will allow us to characterize smaller events recorded only at near-regional distances.
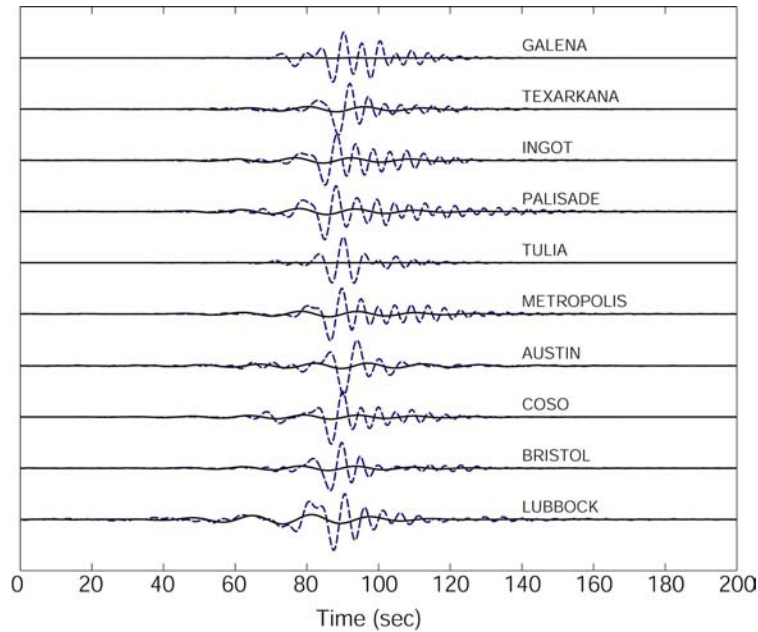
Figure 6. PMF (dashed) extracted Rayleigh waves from Yucca Flat explosions. The solid lines show the PMF data bandpass filtered between 17 and 23 seconds. The explosions TULIA (m_b=3.7) and GALENA (m_b=3.6) did not have measurable surface waves in the 17 to 23 second band at MNV. The data were scaled to the maximum amplitude of each PMF trace.

We will examine the performances of several M_s formulae at near-regional distances during this project, including the Rezapour and Pearce (1998) and Marshall and Basham (1972) equations. Marshall and Basham (1972) reformulated the Prague formula (Vanek *et al.,* 1962) as:

$$M_s = \log_{10} (A_{max}) + B'(\Delta) + P(T) + 0.008h \quad (4)$$

where A_{max} is the maximum Rayleigh wave amplitude (0 to Peak in nm), $B'(\Delta)$ is a distance correction, $P(T)$ is a path correction as a function of period, T, and h is the depth of the event in kilometers. The distance correction (Marshall and Basham, 1972) approximated the $1.66 \log_{10} (\Delta)$ term for distances at large teleseismic differences and was proportional to $0.8 \log_{10} (\Delta)$ for regional distances (Basham, 1971). More recently, a study by Herak and Herak (1993) showed that surface wave amplitudes decrease as $\Delta^{+1.094}$. The path correction is determined from the amplitude of the group velocity (U) dispersion curve predicted by the method of stationary phase (Ewing *et al*., 1957) with the following equation:

$$P(T)= \frac{U}{T^{3/2}\sqrt{\frac{dU}{dT}}} . \quad (5)$$

Marshall and Basham (1972) show $P(T)$ corrections for varying lithospheric structures, however, the authors limited their analyses to periods greater than 10 seconds. We used the group velocity dispersion curves generated from the multiple filter analyses to obtain $P(T)$ for periods between 4 and 10 seconds. For the dominant period (7 sec) of the Yucca Flat explosions shown in Figure 6, the $P(T)$ correction is approximately -0.8 magnitude units (m.u) relative to measurements made at 20 seconds.

We used the Marshall and Basham (1972) formula (Equation 4) and dispersion-curve generated $P(T)$ (equation 5) to calculate preliminary M_s values for both 20 second (Figure 7; circles) and 7 seconds (asterisks) Rayleigh wave data from the Yucca Flat events.   Both the M_s(20) and M_s(7) values show similar trends; however, the M_s(7) values are approximately 0.24 m.u. larger. We plan to examine the source of this discrepancy which could be associated with incorrect attenuation for the near-regional, short-period Rayleigh waves or the difficulties of measuring $P(T)$ near an

Airy phase. We note that Denny *et al*. (1987) used the Marshall and Basham (1972) formula with regional NTS data to improve the separation of earthquake and explosion populations based on the M_s:m_b discriminant. However, they were only able to apply their method to a single explosion with $m_b < 3.8$. Our initial study of only 10 events from the Yucca Flats region have found surface waves for two events at these smaller magnitudes, and we will continue to use the phase match filtering, array processing methods, and other techniques to extract Rayleigh waves from small earthquakes and explosions. Another method of calculating regional M_s for data with periods less than 20 seconds was developed by Woods and Harkrider (1995). In their method, synthetic seismograms are used to establish a relationship between the amplitudes of the regional Rayleigh-wave pulse and associated Rayleigh waves that have propagated to distances of 40°. These methods allowed for the calculation of M_s values for nuclear explosions over a wider magnitude range than previously accomplished. We plan to use their method and compare the synthesized M_s values with ours calculated directly from near-regional measurements of short-period surface waves.
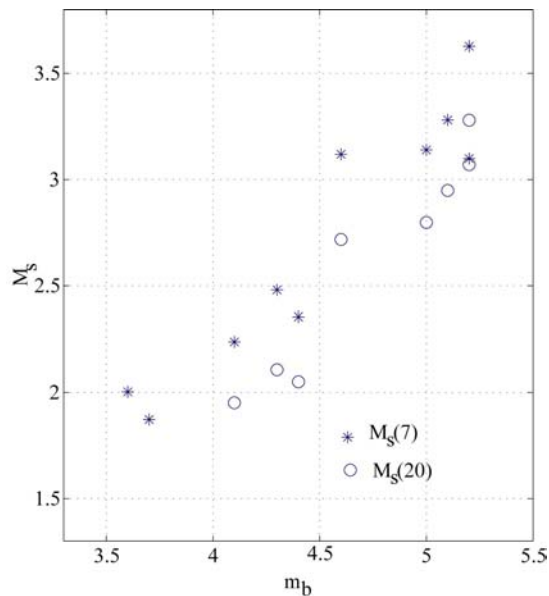
Figure 7. Comparison of M_s values calculated for Yucca Flat explosions using 7 second (asterisks) and 20 second (circles) Rayleigh wave data.

CONCLUSIONS AND RECOMMENDATIONS

Our preliminary dataset has allowed us to calibrate the DTV m_b (Denny *et al.,* 1987) formula for *Pn* arrivals recorded at element NV31, collocated with the historical station MNV. We have determined DTV m_b constants for NV08 and NV32 to calibrate them against corrected DTV m_b measured at element NV31, for events on or near NTS. We observed systematic and consistent underestimation of magnitudes for events on NTS at NV08 and NV31; however, we have not completed results at NV33 because of a limited database. Since, to this date, we found only a small number of suitable earthquakes on and around NTS, these observations remain to be confirmed by a larger collection of events, and thus the results presented within are preliminary and will be updated as more data become available. We have calibrated the *P*g magnitude values measured at NV08, NV31 and NV32 against corrected DTV m_b measured at element NV31. To obtain these magnitude values we found new corrections for distance and new constants.

As a result of NVAR's near-regional distance (less than 250 km) to the Nevada Test Site, the surface waves recorded at this station from events on or near the test site are dominated by an short-period Rayleigh wave with period considerably less than 20 secs. We have used phase match filtering techniques to extract Rayleigh waves from several Yucca Flat explosions, and observed that the 20 second surface waves fall below detection thresholds near m_b=4.1; however, the shorter-period Rayleigh waves are still measurable at m_b=3.7 and lower. These results suggest that the surface wave magnitude scale for this region must be calibrated at these shorter-periods in order to examine the performance of the M_s:m_b discriminant at smaller magnitudes. We plan to compare the direct

measurements to measurements made on synthesized 20 second period data using the technique of Woods and Harkrider (1995).

REFERENCES

Denny, M.D., S.R. Taylor, and E.S. Vergino (1987), Investigation of m_b and M_s formulas for the western United States and their impact on the M_s/m_b discriminant, *Bull. Seism. Soc. Am.* 77, 987.

Denny, M. D. (1998), Mina Seismic Data: Historic background for CTBT Monitoring, UCRL-MI-130657.

Dziewonski, A., S. Bloch, and M. Landisman (1969), A technique for the analysis of transient seismic signals, *Bull. Seism. Soc. Am.* 59, 427.

Evernden, J.F. (1971), Variation of Rayleigh wave amplitude with distance, *Bull. Seism. Soc. Am.* 61, 231.

Ewing, ,W. M., F., Press, and W. S. Jardetsky (1956), *Elastic waves in layered media*, McGraw Hill, New York.

Herak, M. and D. Herak (1993), Distance dependence of M_s and calibrating function for 20 second Rayleigh waves, *Bull. Seism. Soc. Am.* 83, 1681.

Herrin, E. and T. Goforth (1977), Phase-matched filters: application to the study of Rayleigh waves, *Bull. Seism. Soc. Am.* 67, 1259.

Marshall, P.D. and P.W. Basham (1972), Discrimination between earthquakes and underground explosions employing and improved M_s scale, *Geophys. J. R. astr. Soc.,* 28, 431.

Rezapour, M. and R. G. Pearce (1998), Bias in surface-wave magnitude doe to inadequate distance corrections, *Bull. Seism. Soc. Am.,* 88, *43-61.*

von Seggern, D. (1977), Amplitude distance relation for 20-Second Rayleigh waves, *Bull. Seism. Soc. Am.,* 67, 405-511.

Tibuleac, Ileana M. and E. T. Herrin (1997), Calibration studies at TXAR, *Seis. Res. Lett,* 68, 353.

Tibuleac, Ileana M. and E. T. Herrin (2001), Detection and Location Capability at NVAR for events on the Nevada Test Site, *Seis. Res. Lett*., 72, 97.

Tibuleac, I.M., E. T. Herrin and P. Negraru (2001), Calibration studies at NVAR, *Seis. Res. Lett,*72, 754.

Vanek, J., A. Zatopek, V. Karnik, N.V. Kondorskaya, Y.V. Riznichenko, E.F. Savarensky, S.L. Solov'ev, N.V. Shebalin (1962), Standardization of magnitude scales, *Bull. (Izvest.)* Acad. Sci. U.S.S.R., Geophys. Ser., 2, 108.

Woods, B.B. and D.G. Harkrider (1995), Determining surface-wave magnitudes from regional Nevada Test Site data, Geophys. J. Int. 120, 474.